Review

JOURNAL OF COMPOSITE MATERIALS

Journal of Composite Materials
2022, Vol. 0(0) 1–9

DOI: 10.1177/00219983211065206
journals.sagepub.com/home/jcm
SAGE

Mechanical properties of carbon fibre reinforced composites modified with star-shaped butyl methacrylate

Rochele Pinto[1], Gediminas Monastyreckis[1], Hamza Mahmoud Aboelanin[2,3], Vladimir Spacek[4] and Daiva Zeleniakiene[1]

Abstract

This article presents the possibility of strength improvement and energy absorption of carbon fibre reinforced polymer composites by matrix modification. In this study, the mechanical properties of bisphenol-A epoxy matrix and carbon fibre reinforced polymer composites were modified with four different wt.% of star-shaped polymer *n*-butyl methacrylate (P*n*-BMA) block glycidyl methacrylate (PGMA). The tensile strength of the epoxy with 1 wt.% star-shaped polymer showed 128% increase in comparison to unmodified epoxy samples. Two different wt.% were then used for the modification of carbon fibre-reinforced polymer composite samples. Tensile tests and low-velocity impact tests were conducted for characterising modified samples. Tensile test results performed showed a slight improvement in the tensile strength and modulus of the composite. Low-velocity impact tests showed that addition of 1 wt.% star-shaped polymer additives increase composite energy absorption by 53.85%, compared to pure epoxy composite specimens. Scanning electron microscopy (SEM) analysis of post-impact specimens displays fracture modes and bonding between the matrix and fibre in the composites. These results demonstrate the potential of a novel star-shaped polymer as an additive material for automotive composite parts, where energy absorption is significant.

Keywords

star-shaped polymers, carbon fibre composites, tensile, impact

Introduction

Sustainability, fuel efficiency and crashworthiness are the main priorities of today's automotive industries. Ongoing research on composite recyclability has led them to be a viable material for some of the vehicle's construction parts. The cost related to manufacturing could be dramatically reduced using moulding pre-pregs and cheaper fibres.[1] Closed-loop recycling could also make composite more suitable for the automotive industry using resin removal techniques and fibre reusability for less critical (low strength) components such as interior panels and air-intakes.[2] Short-fibre reinforced polymer composites are an excellent choice for bumpers due to their processability, forming flexibility, low price and recyclability.[3] The main components responsible for crashworthiness that could also be switched to composite materials can be chassis, impact beams, hood and roof.[4] Some examples show that carbon fibre reinforced polymer (CFRP) components lead to 10–70% weight savings and up to 42% reduced fuel consumption.[5] Although composites have higher material costs than traditional metals, they compensate for it during the exploitation period due to the vehicle's reduced weight and lower fuel consumption. Carbon fibres (CF) possess low density, high specific strength, electrical conductivity and low coefficient of thermal expansion, while aramid fibres possess high impact resistance.[4] Given the ease of manufacturing of automotive components made of monolithic and traditional materials, fibre-reinforced polymer

[1]Department of Mechanical Engineering, Kaunas University of Technology, Kaunas, Lithuania
[2]Institute of Chemistry and Technology of Macromolecular Materials, Faculty of Chemical Technology, University of Pardubice, Pardubice, Czech Republic
[3]Department of Chemistry, Faculty of Science, Al-Azhar University, Cairo, Egypt
[4]Synpo, Pardubice, Czech Republic

Corresponding author:
Gediminas Monastyreckis, Department of Mechanical Engineering, Kaunas University of Technology, Studentu st. 56, Kaunas 51424, Lithuania.
Email: gediminas.monastyreckis@ktu.edu

composites fall short due to their time-consuming and longer lead times to reach customer demands. To address this shortcoming, high-end automotive companies now look to manufacture composite components as a single piece using 'Toray's High Cycle Resin Transfer Moulding'.[6] Local incorporation of fibre reinforced composites by curing into metallic automotive components serve as an alternative for inflated costs associated with carbon fibre and simultaneously allow consumer-based specific applications.[7] In recent times, patented carbon fibre composites have been introduced that have the ability to carry electrical charge and act as a battery for electric vehicles.[8] Despite these characteristics, reinforcing fibres have a lower scope of composite's impact properties improvement compared to the possibilities of improving through the polymer matrix modification. Properties such as damage tolerance and impact behaviour depend mainly on the matrix's properties and adhesion to fibres. In the automotive industry, the criteria for polymer-matrix composites are processability, durability and high energy absorption.[9] In order to improve matrix properties, various additives and fillers can be used. The most common of them are nanoparticles such as graphenes ,[10] MXene ,[11-12] carbon nanotubes (CNTs)[13] and other flexible additives such rubber particles[14] or star-shaped polymers.[15]

These additives have known to increase the strength of composites. Graphene deposition increased the surface roughness of carbon fibre, causing better bonding between the resin and matrix, and resulted in the shear strength increase from 50 to 72 MPa.[16] Zhao et al. performed carbon fibre reinforced epoxy composite testing with MXene nanosheets coatings.[17] The NH_2-CF/MXenes/EP composites increase the tensile, flexural, shear and impact strength by 40.8%, 45.9%, 38.5% and 74.4%, respectively. The MXene nanosheets act as additional reinforcement for interfacial adhesion, reducing interlaminar stress and increasing the toughness of the carbon fibre.[17] Hybrid composites with aligned nanosheets of graphene and MXene have demonstrated better tensile strength compared to random inclusions of these nanoparticles.[18] In-situ growth of CNTs on individual carbon fibre surface has increased flexural strength by 30% and flexural modulus by up to 70% of the composite.[19] Another research conducted by Hossain et al.[20] obtained polymer matrix flexural strength and modulus increase by 14% and 27%, respectively, when 0.3 wt.% of CNTs were used. Aldajah et al. performed alignment of the CNTs using electrical impulses and obtained a significant increase in flexural modulus by 46% compared to the non-aligned tubes.[21] Core-shell rubber particles (MX-136) mixed with epoxy matrix showed up to 87% increase in the impact strength when compared to pure epoxy samples.[22]

Star-shaped polymers which have multiple arms connected to one central core are attractive because of their important properties such as smaller hydrodynamics, lower solution and melt viscosities compared to linear polymers of the same molar mass,[23] which facilitate coating, extrusion, improving of carbon fibre reinforced resin composite properties or other manufacturing processes. Star-shaped polymers can be synthesised via controlled/living polymerisation such as Group Transfer Polymerisation (GTP)[24] has increased rapidly as its applicability for different acrylic monomers, and it operates at room temperature and above. The main two methods that are generally followed in the preparation of star-shaped polymers via GTP: core-first[25] and arm-first.[26] The core-first method involves reacting living chains with a multifunctional initiator, and the number of arms of each star-shaped polymer is determined by the initiating functionalities on each initiator. However, the multifunctional initiator must be previously synthesised, which is difficult and expensive. The arm-first method consists of a reacting-preformed linear macromolecule initiator (MI) with a cross-linker. Polyhedral Oligomeric Silsesquioxane (POSS) star-shaped polymer showed an increase of interfacial shear strength (IFSS) of the composites by up to 31.5%, due to improved interfacial adhesion between the fibres and the matrix.[27] Another experiment was conducted on the use of POSS as a novel coupling agent between the carbon fibre matrix and epoxy for the functionalisation of traditional carbon fibres, resulting in improvement in the polarity and roughness of the fibre surface and increase in the composite's IFSS by improving the wettability properties and bonding.[28] Zhang. et al. analysed interlaminar shear strength (ILSS) using methacrylic-POSS coating for CF. Due to uniform load transfer from the matrix to fibres, ILSS of the composite increased by 34%.[29]

Poly (methyl methacrylate) (PMMA) composites formed in the presence of star polymers behaving as shape memory polymers have been shown to increase the thermo-mechanical properties of the composite. The star polymers were vital in improving the shape memory abilities of the polymer network.[30] Increase in amounts of star polymer has shown to increase the handling of external stress in polymer network due to better cross-linking properties.[31] Star polymers created by reversible addition-fragmentation chain transfer (RAFT) are shown to improve the mechanical properties of epoxy thermosets due to the formation of nanoparticles by cross-linking.[32] Hyper star polymers formed with PMMA and poly-hydroxylmethacrylate participated in the curing process but and increased toughness due to 'nanograined morphology'.[33]

This work aims to investigate the mechanical properties of carbon fibre epoxy composites with matrix modified by a novel GTP 475 star-shaped polymer *n*-butyl methacrylate (P*n*-BMA) block glycidyl methacrylate (PGMA). The improved composites can be applied in various automotive components that require higher safety and impact absorption.

Materials and methods

Materials

n-butyl methacrylate (99%, Sigma-Aldrich, United States) and glycidyl methacrylate (97%, Sigma-Aldrich, United States) were purified by passing through a column filled with alumina to remove inhibitors and tetrahydrofuran (99.8%, VWR Chemicals, United States) was also dried by passing through a column filled with alumina. Methyl trimethylsilyl dimethyl ketene acetal and tetrabutylammonium acetate were purchased from Sigma-Aldrich and used without further purification. CHS Epoxy 582 ™ (bisphenol A) matrix and Telalit 0420 ™ (diamine) hardener (mixing ratio of 100:25), supplied by Spolchemie (Czech Republic), were used for the preparation of the matrix. To fabricate the fibre–reinforced composites, twill-woven 2/2 carbon fabric Interglas 92,110 (Porcher Industries, Erbach, Germany) of density 160 g/m^2 with filament diameter of 7 μm was used.

Synthesis of GTP 475 (Pn-BMA-block co-PGMA star-shaped polymer)

Group Transfer Polymerisation 475 was synthesised via GTP technique through the 'one pot' arm-first method. The weight ratio of monomers to tetrahydrofuran (THF) is 1:1. A dry three-neck bottom flask with a magnetic stir bar was degassed and backfilled with nitrogen during the polymerisation process THF as solvent and glycidyl methacrylate (2 units) and *n*-butyl methacrylate (28 units) monomers were added dropwise. Glycidyl methacrylate was chosen to be a comonomer in our polymer because it has an epoxy group that can react with hardener and be built in the epoxy polymer network of the composite matrix. After stirring for 20 min 10 mL of the mixture, arm sample, was removed for further characterisation by gel permeation chromatography (GPC). Finally, we add EGDMA cross-linker to the mixture and let the mixture stir for about 40 min. The star-shaped polymer was stored in 50% THF solution for further characterisation and as additives against delamination occurring in composites.

Characterisation of star-shaped polymer

The number average molecular weight (M_n), weight average molecular weight (M_w), Z average molecular weight (M_z) and its polydispersity (M_w/M_n) of the P*n*-BMA-block co-PGMA arm and star-shaped polymer are characterised by gel permeation chromatography was performed using Waters eAlliance 2695 separation system with a refractive index detector 2410. Two PLgel Mixed-C 300 × 7.5 mm columns were used with tetrahydrofuran as a mobile phase at 1 mL/min. The column calibration was done by polystyrene standards covering the molecular weight of 162 g/mol to 6,000,000 g/mol.

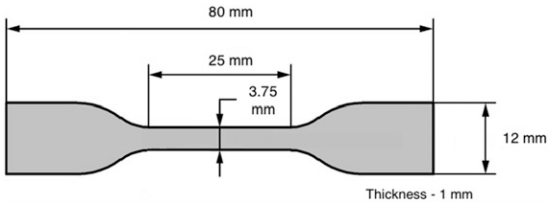

Figure 1. Dog-bone mould dimensions.

Specimen preparation and mechanical testing

Four different wt. % of GTP 475 were chosen – 1%, 3%, 5% and 7% to incorporate in the epoxy to configure optimum loading. Dog-bone shaped moulds were prepared according to ISO 527-2-5A with dimensions shown in Figure 1. The epoxy and stars were mixed, resulting in a highly viscous solution. The mixture was heated above the temperature of the boiling point of THF (66°C) to evaporate the solvent and reduce the viscosity. On evaporation of THF, the temperature was lowered to below 60°C, to ensure that the curing process did not occur prematurely on the addition of the hardener. After the addition of the hardener, the epoxy mixture was then degassed in the vacuum chamber for 5–10 min, after which it was poured into the moulds. After placing the moulds at room temperature overnight, they were cured in the oven for 2 h at 60°C, 1 h at 80°C and 1 h at 120°C.

The CFRP composites were prepared using the vacuum-assisted hand lay-up technique. Five layers of carbon fibre were used to fabricate the composites of thickness 1 mm. Subsequently, the lay-up was vacuum bagged and left to cure for 24 h at room temperature. The samples were then cured in the oven for 2 h at 60°C, 1 h at 80°C and 1 h at 120°C. The samples were machined and smaller samples of desired dimensions for further testing were cut out.

Tensile tests specimens for epoxy resin were prepared according to ISO 527-2-5A standard. Five samples of each loading (pure epoxy, 1, 3, 5 and 7 wt.%) were prepared. Two different loadings of GTP 475 (1 and 3 wt.%) were reinforced by carbon fibre. The loadings were chosen according to the tensile tests performed on the epoxy specimens and exhibited a higher possibility in the improvement of properties compared to other loadings. CFRP specimens (250 mm × 25 mm) were prepared according to ASTM D3039 standard. Abrasive material was used for end tabs to avoid slippage in the grips. The testing was performed using H10 KT and H50 KT universal column testing machine (Tinius Olsen, UK), with a crosshead strain rate of 2 mm/min for both epoxy and composite specimens.

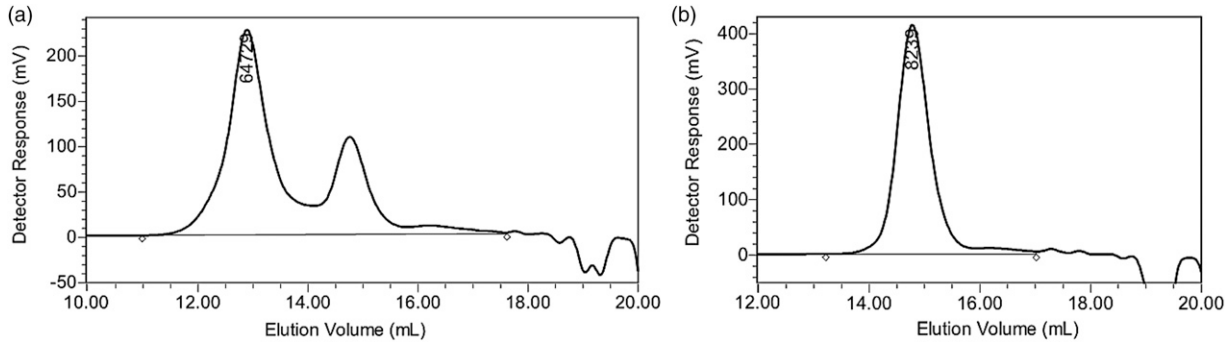

Figure 2. GPC chromatogram results of (a) star core and (b) free arms.

Low-velocity instrumented puncture tests were performed on five-layer CF laminate according to ISO 6603-2, using an impact tower machine (Coesfeld GmbH & Co. KG, Germany). The mass and diameter of the impactor head was 5.185 kg and 20 mm, respectively, and dropped from a height of 0.4 m. The impact velocity recorded was 2.80 m/s. The experiments were conducted at room temperature. From the force-time graph, acceleration was calculated. Double integration of the acceleration provided the displacement at every time interval.

The fracture behaviour, adhesive and cohesive failure of the CFRP samples post-impact modified with 1 and 3 wt.% GTP 475 were characterised using scanning electron microscopy (SEM) (Hitachi S-3400N, Japan). Fractured carbon fibre specimens were taken from the damaged area of the samples after the impact test. The images of the samples were captured under a high vacuum and an accelerating voltage of 3 kV.

Table 1. GPC results of GTP 475 star-shaped polymer.

	M_n	M_w	M_z	*Polydispersity* (M_w/M_n)
Star core	12,200	50,700	89,800	4.17
Free arms	6500	8200	9400	1.25

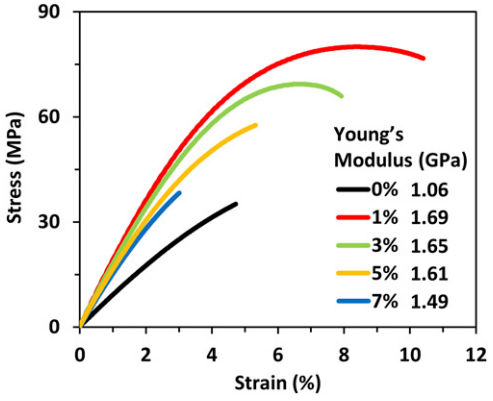

Figure 3. Average tensile results of epoxy specimens with various wt.% of GTP 475.

Results

Gel permeation chromatography

Gel permeation chromatography was performed to determine the average molecular weight and concentration of the star core and free arms in the solution. GPC is a type of size exclusion chromatography where the polymer dissolved in a solution is made to elute a column packed with porous material (polystyrene). The porosity of the packing material causes the smaller sized molecules to permeate deeper into the smaller pores while the larger sized molecules are excluded from pores with size smaller than the size of molecules by diffusion effect, the large molecules elute from the column first then followed by the molecules decreasing molecular size.[25] As shown in Figure 2(a) two peaks the first peak is related to star-shaped polymer with M_n = 12,200, and the second peak is to the arms, which is shown clearer in Figure 2(b) with M_n = 6500. We found the star-shaped polymer with a high molecular weight eluted at lower elution volume (13 mL) while the arm with a lower molecular weight than star-shaped polymer eluted at higher elution volume (15 mL). This process helps determine the average molecular weights and concentration of the molecules by observing their elution volume. A refractive index detector is placed at the end of the column to detect the concentration of polymer in the solution by the difference in their refractive indices. The results of GPC performed on GTP 475 are displayed in Table 1.

In Table 1, M_n is the total weight of the polymer divided by the number of molecules; M_w – average molecular weight. It is the mass of the individual chains that makes up the overall weight of the polymer; M_z, M_{z+1} – average

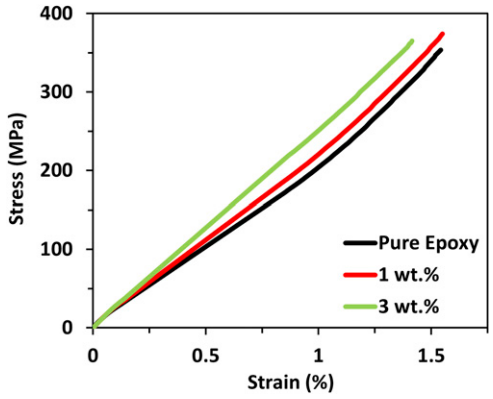

Figure 4. Average tensile results of CFRP samples with pure epoxy, 1 wt.% and 3 wt.% GTP 475.

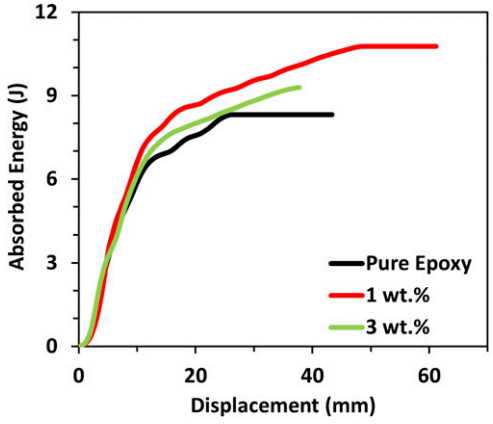

Figure 5. Average low-velocity impact results of CFRP samples with pure epoxy, 1 wt.% and 3 wt.% GTP 475.

molecular weight with a number of chains 2 and 3, respectively; *MP* – molecular weight of the highest peak. Polydispersity – (M_w/M_n) is an index for the distribution of the polymer chain within the polymer. All weights are expressed in g/mol. The results of polydispersity of arms of methyl methacrylate star polymers synthesised by process of GTP using the arm-first technique are comparable to the ones previously reported.[34,35]

Tensile tests

Tensile tests were performed to analyse the optimum percentage of stars on the strength of the epoxy matrix (Figure 3). The tensile modulus of each wt.% sample was calculated at 0.25–0.2% strain region. The tensile modulus gradually decreases with increase in the wt.% of GTP 475. The elongation observed is the highest in epoxy loaded with 1 wt.% GTP 475. The optimum wt.% addition of was found to be 1 wt.% with a maximum stress value of 79.99 MPa with an improvement of 128% in strength compared to pure epoxy. Due to the increase in viscosity with the addition of higher amounts of the stars, micro-defects such as air bubbles caused specimens to break earlier.

The tensile strength at the break for CFRP samples with pure epoxy, 1 and 3 wt.% GTP 475 was observed to be 353 MPa, 374 MPa and 365 MPa, respectively (Figure 4). The modified CFRP specimens also showed a slight improvement in the tensile modulus with the optimum loading. Nearly every specimen broke in a LAT manner (Lateral, At grip and Top). Higher elongation of the CFRP samples with pure epoxy shows that with the addition of GTP 475, the brittle behaviour is increased, leading to lower strains produced on tensile loading.

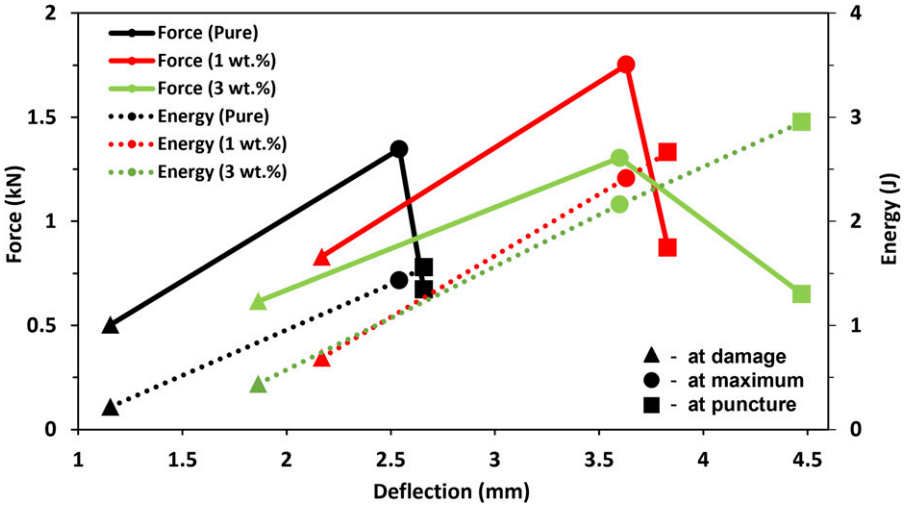

Figure 6. Low-velocity impact test results. Impact energy and force against displacement.

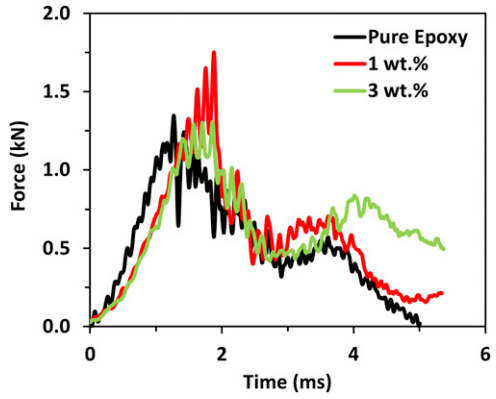

Figure 7. Force-time plots for CFRP samples with pure epoxy, 1 wt.%, and 3 wt.% GTP 475.

Low-velocity impact tests

Carbon fibre reinforced polymer specimens with 1 and 3 wt.% GTP 475 additive were investigated under impact loading. The impact specimens were punctured under a low-impact mode. The specimens performed well under impact, and out of the total impact energy of 20 J, which was applied on the specimens, 10.77 J, 9.29 J 8.31 J were absorbed by the 1 wt.%, 3 wt.% and pure CFRP composites, respectively (Figure 5). Scanning electron microscopy analysis also approved that no major damage was seen on the 1 wt.% specimens indicating good bonding between fibres and matrix and the increase in absorbed energy.

The specimens' deflection at puncture is 2.66 mm, 4.48 mm and 3.83 mm for pure, 1 wt.% and 3 wt.% CFRP,

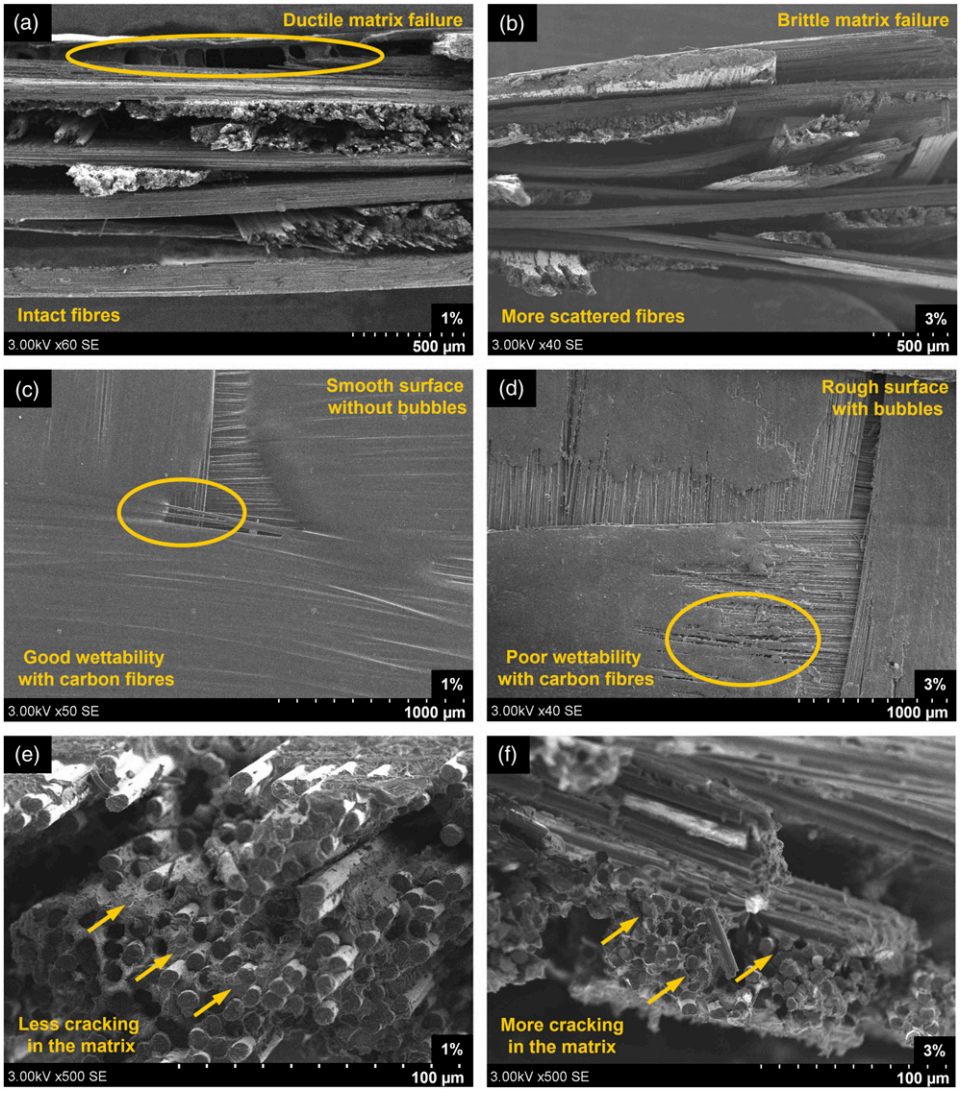

Figure 8. Comparison of SEM images of post-impact results of carbon fibre composite modified with 1 wt.% and 3 wt.% of GTP 475. (a, b) interlaminar failure; (c, d) top surface of the sample (non-damaged area); (e, f) magnified region of fractured carbon fibres and adhered matrix after the impact test.

respectively. The forces required at puncture is higher in the case of the stars, showing higher impact strength (Figure 6). From Figure 6, it can be observed that deflection caused in the GTP 475 specimens is higher, exhibiting better energy-absorbing properties. The boundary shape of the impact event was small, while the rest of the specimen remained intact with no damage. Plots shown in Figure 7 indicate both specimens underwent brittle fracture.[36] As observed, the area under the curve for the force-time plot for 1 wt.% GTP 475 is greater than that of pure epoxy, indicating higher energy absorption.

Scanning electron microscopy characterisation

Scanning electron microscopy analysis was performed to study the failure behaviour of carbon fibres caused by impact loading. In Figure 8, composite pieces of the damaged (punctured) areas were carefully cut and analysed in various magnifications. Figure 8(a) shows good bonding between the fibres and epoxy matrix and high ductility epoxy trances between the debonded plies in composites modified by 1 wt.% of GTP 475. Also, despite the delamination between the plies, most of the fibres remained intact with each other. Delamination produced due to high interlaminar fracture is observed in the case of 3 wt.% of GTP in Figure 8(b). Figure 8(c) shows carbon fibres with partly wetted areas and no trace of air bubbles due to lower viscosity of 1 wt.% samples. The 3 wt.% GTP 475 matrix shows traces of microbubbles, and poor wettability with the fibres, due to higher viscosity and surface tension (Figure 8(d)). In Figure 8(e), good bonding between the matrix and fibres is observed. The matrix strongly adhered to the laminates, leaving rough cohesive matrix failures. Furthermore, almost no debonding and cracking is observed due to the high flexibility of the matrix, good adhesion and transfer of the loads between the fibres. In Figure 8(f), several cases of adhesive failure and fibre pull out are observed, showing stiffness of the matrix. The surface of the samples showed matrix cracking and shear waves caused to impact.

Conclusions

Experimental investigations were carried out to observe the effects of star-shaped polymer GTP 475 additives on the epoxy matrix (Bisphenol-A) and carbon fibre composites. Tensile and impact tests were performed to analyse the matrix modification influence. Tensile tests performed on epoxy with various weight fractions of GTP 475 showed that the addition of 1 wt.% is optimum. The tensile strength was improved from 35.09 MPa (for pure epoxy) to 79.99 MPa (for 1 wt.% modified epoxy). Carbon fibre was reinforced with 1 wt.% and 3 wt.% modified epoxy matrix. The tensile tests showed slight but not significant improvements in modulus and strength. The low-velocity impact tests showed higher deflection and more energy-absorbing results in GTP 475 modified samples compared to pure CFRP composites. The 1 wt.% samples absorbed more energy while having lower deflection, compared to 3 wt.% samples showing scope for further energy absorption. SEM characterisation was performed to investigate failure modes and adhesion behaviour of the composite specimens under impact loading. Both 1 and 3 wt.% exhibited brittle modes of failure with evident fibre pull out without dimpling. 1 wt.% of GTP 475 CFRP samples showed good adhesion, wettability and several cases of matrix bridging were observed. CFRP samples modified with 3 wt.% exhibited stiffness and cracks throughout the cured matrix.

These results demonstrate the potential of GTP 475 star-shaped polymer as a suitable additive, highly influencing impact properties of carbon fibre-reinforced polymer composites. Furthermore, as the stars have great energy-absorbing properties, it has high perspectives for the application in automotive composite components related to durability and crashworthiness.

Declaration of conflicting interests

The author(s) declared no potential conflicts of interest with respect to the research, authorship, and/or publication of this article.

Funding

The author(s) disclosed receipt of the following financial support for the research, authorship, and/or publication of this article: This work was developed under the M-Era.Net 2 research project entitled EPIC - European Partnership for Improved Composites, No. TH06020001.

ORCID iD

Gediminas Monastyreckis https://orcid.org/0000-0003-2067-5542

References

1. Fukuda H and Chou T-W. A probabilistic theory of the strength of short-fibre composites with variable fibre length and orientation. *J Mater Sci* 1982; 17: 1003–1011. DOI: 10.1007/BF00543519.
2. Ishikawa T, Amaoka K, Masubuchi Y, et al. Overview of automotive structural composites technology developments in Japan. *Composites Sci Technology* 2018; 155: 221–246. DOI: 10.1016/j.compscitech.2017.09.015.
3. Rezaei F, Yunus R, Ibrahim NA, et al. Development of short-carbon-fiber-reinforced polypropylene composite for car bonnet. *Polymer-Plastics Technology Eng* 2008; 47: 351–357. DOI: 10.1080/03602550801897323.
4. Applications M and Fibers M. *High Performance and Specialty Fibers*, Tokyo: Springer, 2016. DOI: 10.1007/978-4-431-55203-1.

5. Shanmugam K, Gadhamshetty V, Yadav P, et al. Advanced high-strength steel and carbon fiber reinforced polymer composite body in white for passenger cars: environmental performance and sustainable return on investment under different propulsion modes. *ACS Sustainable Chem Eng* 2019; 7(5): 4951–4963. DOI: 10.1021/acssuschemeng.8b05588.
6. Stewart R. Rebounding automotive industry welcome news for FRP. *Reinforced Plastics* 2011; 55: 38–44. DOI: 10.1016/S0034-3617(11)70036-4.
7. Thomas R, Wehler S and Fischer F. Predicting the process-dependent material properties to evaluate the warpage of a co-cured epoxy-based composite on metal structures. *Composites A: Appl Sci Manufacturing* 2020; 133: 105857. DOI: 10.1016/J.COMPOSITESA.2020.105857.
8. Stewart R. Automotive composites offer lighter solutions. *Reinforced Plastics* 2010; 54: 22–28. DOI: 10.1016/S0034-3617(10)70061-8.
9. Manohar DM. Polymer engineering PEB3213. *Polym Composites Eng*; 1: 1–22.
10. Steinke K, Groo L and Sodano HA. Laser induced graphene for in-situ ballistic impact damage and delamination detection in aramid fiber reinforced composites. *Composites Sci Technology* 2021; 202: 108551. DOI: 10.1016/J.COMPSCITECH.2020.108551.
11. Gogotsi Y and Anasori B. The rise of MXenes. *ACS Nano* 2019; 13: 8491–8494. DOI: 10.1021/ACSNANO.9B06394.
12. Zukiene K, Monastyreckis G, Kilikevicius S, et al. Wettability of MXene and its interfacial adhesion with epoxy resin. *Mater Chem Phys* 2021; 257: 123820. DOI: 10.1016/J.MATCHEMPHYS.2020.123820.
13. Yildiz K, Gürkan İ, Turgut F, et al. Fracture toughness enhancement of fuzzy CNT-glass fiber reinforced composites with a combined reinforcing strategy. *Composites Commun* 2020; 21: 100423. DOI: 10.1016/J.COCO.2020.100423.
14. Kinloch AJ, Mohammed RD, Taylor AC, et al. The interlaminar toughness of carbon-fibre reinforced plastic composites using 'hybrid-toughened' matrices. *J Mater Sci* 2006; 41: 5043–5046. DOI: 10.1007/S10853-006-0130-8.
15. Tkachenko IM, Ledin PA, Shevchenko VV, et al. Mixed star-shaped POSS-based molecule with hydroxy group-containing units and azobenzene fragments as two types of arms. *Mendeleev Commun* 2021; 31: 27–29. DOI: 10.1016/J.MENCOM.2021.01.007.
16. He R, Chang Q, Huang X, et al. Improved mechanical properties of carbon fiber reinforced PTFE composites by growing graphene oxide on carbon fiber surfaceber reinforced PTFE composites by growing graphene oxide on carbon ber surface. *Compos Inter* 2018; 25: 995–1004. DOI: 10.1080/09276440.2018.1451677.
17. Zhao X, Qi S, Liu J, et al. Preparation and mechanical performances of carbon fiber reinforced epoxy composites by MXene nanosheets coating. *J Mater Sci Mater Elect* 2019; 30: 10516–10523. DOI: 10.1007/s10854-019-01395-w.
18. Kilikevičius S, Kvietkaitė S, Mishnaevsky L, et al. Novel hybrid polymer composites with graphene and MXene nano-reinforcements: computational analysis. *Polymers* 2021; 13: 1013. DOI: 10.3390/polym13071013.
19. Xiao P, Lu XF, Liu Y, et al. Effect of in situ grown carbon nanotubes on the structure and mechanical properties of unidirectional carbon/carbon composites. *Mater Sci Eng A* 2011; 528: 3056–3061. DOI: 10.1016/j.msea.2010.11.067.
20. Hossain M, Chowdhury M, Salam M, et al. Enhanced mechanical properties of carbon fiber/epoxy composites by incorporating XD-grade carbon nanotube. *J Compos Mater* 2015; 49: 2251–2263. DOI: 10.1177/0021998314545186.
21. Aldajah S and Haik Y. Transverse strength enhancement of carbon fiber reinforced polymer composites by means of magnetically aligned carbon nanotubes. *Mater Des* 2012; 34: 379–383. DOI: 10.1016/j.matdes.2011.07.013.
22. Giannakopoulos G, Masania K and Taylor AC. Toughening of epoxy using core-shell particles. *J Mater Sci* 2011; 46: 327–338. DOI: 10.1007/S10853-010-4816-6.
23. Peleshanko S and Tsukruk VV. The architectures and surface behavior of highly branched molecules. *Prog Polym Sci* 2008; 33: 523–580. DOI: 10.1016/J.PROGPOLYMSCI.2008.01.003.
24. Gao H and Matyjaszewski K. Modular approaches to star and miktoarm star polymers by ATRP of cross-linkers. *Macromolecular Symposia* 2010; 291-292: 12–16. DOI: 10.1002/masy.201050502.
25. Ueda J, Matsuyama M, Kamigaito M, et al. Multifunctional initiators for the ruthenium-mediated living radical polymerization of methyl methacrylate: Di- and trifunctional dichloroacetates for synthesis of multiarmed polymers. *Macromolecules* 1998; 31: 557–562. DOI: 10.1021/MA970476B.
26. Pasquale AJ and Long TE. Synthesis of star-shaped polystyrenes via nitroxide-mediated stable free-radical polymerization. *J Polym Sci A: Polym Chem* 2001; 39: 216–223. DOI: 10.1002/1099-0518.
27. Zhao F and Huang Y. Improved interfacial properties of carbon fiber/epoxy composites through grafting polyhedral oligomeric silsesquioxane on carbon fiber surface. *Mater Lett* 2010; 64: 2742–2744. DOI: 10.1016/j.matlet.2010.08.074.
28. Zhao F and Huang Y. Grafting of polyhedral oligomeric silsesquioxanes on a carbon fiber surface: novel coupling agents for fiber/polymer matrix composites. *J Mater Chem* 2011; 21: 3695–3703. DOI: 10.1039/c0jm03128c.
29. Zhang X, Huang Y, Wang T, et al. Effects of silsesquioxane coating structure on mechanical interfacial properties of carbon fibre/polyarylacetylene composites. *J Mater Sci* 2007; 42: 5264–5271. DOI: 10.1007/s10853-006-0349-4.
30. Liu T, Li J, Pan Y, et al. A new approach to shape memory polymer: design and preparation of poly(methyl methacrylate)

composites in the presence of star poly(ethylene glycol). *Soft Matter* 2011; 7: 1641. DOI: 10.1039/c0sm01401j.

31. Rauschendorfer JE, Möckelmann J, Vana P, et al. Enhancing the mechanical properties of matrix-Free poly(Methyl Acrylate)-grafted montmorillonite nanosheets by introducing star polymers and hydrogen bonding moieties. *Wiley Libr* 2021; 306: 2100054. DOI: 10.1002/mame.202100054.
32. Francis R and Baby DK. A reactive polystyrene-block-polyisoprene star copolymer as a toughening agent in an epoxy thermoset. *Springer* 2016; 294: 565–574. DOI: 10.1007/s00396-015-3810-6.
33. Belmonte A, Däbritz F, Ramis X, et al. Cure kinetics modeling and thermomechanical properties of cycloaliphatic epoxy-anhydride thermosets modified with hyperstar polymers. *J Polym Sci B: Polym Phys* 2014; 52: 1227–1242. DOI: 10.1002/POLB.23555.
34. Themistou E and Patrickios CS. Synthesis and characterization of star polymers and cross-linked star polymer model networks containing a novel, silicon-based. *Macromolecules* 2004; 37: 6734–6743. DOI: 10.1021/ma049618.
35. Kafouris D, Themistou E and Patrickios CS. Synthesis and characterization of star polymers and cross-linked star polymer model networks with cores based on an asymmetric, hydrolyzable dimethacrylate cross-linker. *Chem Mater* 2006; 18: 85–93. DOI: 10.1021/cm051604a.
36. Ozkoc G, Bayram G, Bayramli E, et al. Impact essential work of fracture toughness of ABS/polyamide-6 blends compatibilized with olefin based copolymers. *J Mater Sci* 2008; 43: 2642–2652. DOI: 10.1007/s10853-008-2483-7.